An investigation of heat and mass transfer between air and desiccant film in an inclined parallel and counter flow channels

A. Ali [a], K. Vafai [b,*]

[a] Department of Mechanical Engineering, Ohio State University OSU, Columbus, OH 43210, USA
[b] Department of Mechanical Engineering, University of California at Riverside UCR, A363 Bourns Hall, Riverside, CA 92521 0425, USA

Abstract

Heat and mass transfer between air and falling desiccant film is investigated for inclined parallel and counter flow configurations. Two different configurations are proposed and parametrically analyzed. Effect of inclination angle is examined to study enhancements in dehumidification and cooling processes of the air and regeneration of liquid desiccant in terms of pertinent parameters. Cu-ultrafine particles are also added to the desiccant film to investigate the enhancement in heat and mass transfer between the air and the desiccant film. The pertinent parameters are air and desiccant Reynolds numbers, inlet conditions for both air and liquid desiccant, Cu-ultrafine particles volume fraction, and thermal dispersion. It is shown that inclination angle plays a significant role in enhancing the dehumidification, cooling, and regeneration processes.
© 2003 Elsevier Ltd. All rights reserved.

1. Introduction

Desiccant cooling systems have received much attention in the past couple of decades. Liquid desiccant is brought into contact with air at a low temperature to dehumidify the air. Liquid desiccant is brought again into contact with air at high temperature to regenerate the liquid desiccant. These two processes can be used with conventional air-conditioning to improve the overall performance especially at hot and humid environments. The use of liquid desiccant enhances the indoor air quality, reduces energy consumption, and produces an environmentally safe product [1–3]. Lof [4] initiated the idea of dehumidification in 1955. Chraibi [5] investigated the dehumidification process between air and liquid desiccant on a trickle exchanger. It was found

that a ventilated pad could be used to extract up to 5 kg of water vapor per hour under greenhouse climate conditions. Al-Farayedi et al. [6] studied the heat and mass transfer between air and liquid desiccant in a gauze-type structured packing tower. Three different types of liquid desiccant are compared. It was found that the mixture of calcium chloride and lithium chloride has a significant increase in the mass transfer coefficient compared with the other two solutions. In a recent study, Ali et al. [7,8] analyzed a comparative study between air and desiccant film in parallel and counter flow configurations as well as a cross flow arrangement. It was found that a decrease in air Reynolds number and an increase in the channel height provide better dehumidification and cooling processes for the air.

In the dehumidifier, both air and desiccant film enter the dehumidifier at low temperature. The water vapor content is transferred from the air to the desiccant film. The air is also cooled down because the desiccant film enters at lower temperature than the air. In the regenerator, both desiccant film and air enter the regenerator

* Corresponding author. Tel: +1-909-787-2135; fax: +1-909-787-2899.
  E-mail address: vafai@engr.ucr.edu (K. Vafai).

Nomenclature

C	concentration of desiccant film (kg_w/kg_{sol})
c_p	specific heat at constant pressure (J/kg K)
d_s	average diameter of ultrafine particles (nm)
D	diffusion coefficient (m²/s)
g	gravitational acceleration (m/s²)
H	channel height (m)
h_{fg}	latent heat of vaporization (J/kg)
k	thermal conductivity (W/m² °C)
L	length (m)
$\dot{m}$	mass flow rate (kg/s m)
N	number of ultrafine particles per unit volume
p	pressure (pa)
Re	Reynolds number
T	temperature (°C)
u	velocity in the axial direction (m/s)
V	volume (m³)
W	humidity ratio of the air (kg_w/kg_a)
x	x-coordinate
y	y-coordinate
Z	salt concentration in the desiccant film (kg_{salt}/kg_{sol})

Greek symbols

λ	coefficient of thermal dispersion (m)
ρ	density (kg/m³)
μ	dynamic viscosity (N s/m²)
θ	inclination angle (°)
ψ	stream function (m²/s)
α	thermal diffusivity (m²/s)
δ	thickness (m)
ξ	variable transformation in the x-direction
η	variable transformation in the y-direction
υ	velocity in transverse direction (m/s)
ϕ	volume fraction (%)
Ω	vorticity (s⁻¹)

Subscripts

a	air
CF	counter flow
d	desiccant
dis	dispersion
eff	effective value
f	fluid
i	inlet conditions
int	interfacial condition between air and desiccant film
m	mean value
o	outlet condition
PF	parallel flow
s	Solid
sol	desiccant film
t	total pressure
ws	saturation pressure
z	vapor pressure

at high temperature and water vapor is transferred from the film to the air. Therefore, a continuous loop of dehumidification of the air and regeneration of desiccant film can be achieved.

The addition of Cu-ultrafine particles (nanoparticles) to any fluid is expected to boost heat and mass transfer within the solid–liquid mixture. Number of studies [9–11] has focused in the addition of these ultrafine particles to a working fluid to measure the thermal conductivity of this new nanofluid. Xuan and Roetzel [12] proposed two different approaches to predict the thermal conductivity of nanofluids. Both approaches are utilized in this study.

In this study, heat and mass transfer between air and desiccant film in inclined parallel and counter channels is investigated. Four categories are considered in this work: (1) low air Reynolds number for the inclined parallel flow channel; (2) low air Reynolds number for the inclined counter flow arrangement; (3) high air Reynolds number for inclined parallel flow channel; and (4) high air Reynolds number for counter flow configuration. After considering the four categories, this study will focus on high air Reynolds number for inclined

parallel flow channel. Effect of inclination angle will be discussed in terms of pertinent parameters such as air and desiccant Reynolds numbers, inlet air conditions, desiccant inlet conditions, Cu-ultrafine particles volume fraction of the desiccant film, and thermal dispersion. In addition, pertinent categories are used to compare the effect of inclination angle on heat and mass transfer between air and desiccant film.

2. Mathematical formulation

The inclined parallel and counter flow channels between air and desiccant film are shown in Fig. 1(a) and (b), respectively. Note that the inclination angle is considered inward for the parallel flow channel and outward for the counter flow configuration: l_1 is unchanged for both flow channels and l_2 is reduced for parallel flow and increased for the counter flow as the angle increases. The assumptions for this analysis are (1) flow is laminar and steady state, (2) thermal properties of the air and the desiccant film are constant except for the thermal conductivity of the desiccant film, (3) gravitational force on
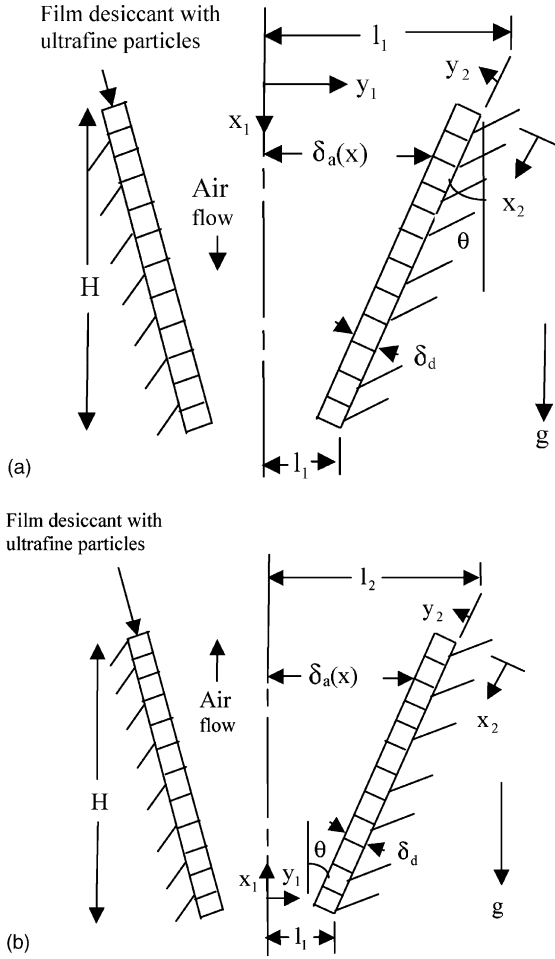
Fig. 1. Schematic of inclined (a) parallel and (b) counter flow configurations.

the air is neglected, (4) film thickness is taken to be constant, (5) thermodynamic equilibrium exists at the interface between air and the desiccant film. The general model for continuity, momentum, energy, and mass diffusion for air for both flow channels is given by

$$\frac{\partial u_a}{\partial x_1} + \frac{\partial v_a}{\partial y_1} = 0 \tag{1}$$

$$\rho_a \left(u_a \frac{\partial u_a}{\partial x_1} + v_a \frac{\partial u_a}{\partial y_1} \right) = -\frac{\partial p}{\partial x_1} + \mu_a \left(\frac{\partial^2 u_a}{\partial y_1^2} \right) \tag{2}$$

$$\rho_a \left(u_a \frac{\partial v_a}{\partial x_1} + v_a \frac{\partial v_a}{\partial y_1} \right) = -\frac{\partial p}{\partial y_1} + \mu_a \left(\frac{\partial^2 v_a}{\partial y_1^2} \right) \tag{3}$$

$$\rho_a c_p \left(u_a \frac{\partial T_a}{\partial x_1} + v_a \frac{\partial T_a}{\partial y_1} \right) = k_a \left(\frac{\partial^2 T_a}{\partial y_1^2} \right) \tag{4}$$

$$u_a \frac{\partial W}{\partial x_1} + v_a \frac{\partial W}{\partial y_1} = D_a \left(\frac{\partial^2 W}{\partial y_1^2} \right) \tag{5}$$

Coordinate transformations are needed to solve the governing equations for the air. The following equations will be used to perform the coordinate transformation:

$$\xi = x_1 \quad \text{and} \quad \eta = \frac{y_1}{\delta_a(x_1)} \tag{6}$$

where

$$\delta_a(x_1) = l_1 - x_1 \tan \theta$$
for the inclined parallel flow channel (7)

$$\delta_a(x_1) = l_1 + x_1 \tan \theta$$
for the inclined counter flow channel (8)

The general transformed mass, momentum, energy, and mass diffusion equations for air in the inclined parallel flow channel become as follows:

$$\left(\frac{\partial u_a}{\partial \xi} + \frac{\eta \tan \theta}{\delta_a(x_1)} \frac{\partial u_a}{\partial \eta} \right) + \frac{1}{\delta_a(x_1)} \frac{\partial v_a}{\partial \eta} = 0 \tag{9}$$

$$\rho_a \left(u_a \frac{\partial u_a}{\partial \xi} + \frac{v_a + \eta \tan \theta u_a}{\delta_a(x_1)} \frac{\partial u_a}{\partial \eta} \right)$$
$$= -\frac{\partial p}{\partial \xi} + \frac{\mu_a}{\delta_a^2(x_1)} \left(\frac{\partial^2 u_a}{\partial \eta^2} \right) \tag{10}$$

$$\rho_a \left(u_a \frac{\partial v_a}{\partial \xi} + \frac{v_a + \eta \tan \theta u_a}{\delta_a(x_1)} \frac{\partial v_a}{\partial \eta} \right)$$
$$= -\frac{\partial p}{\partial \eta} + \frac{\mu_a}{\delta_a^2(x_1)} \left(\frac{\partial^2 v_a}{\partial \eta^2} \right) \tag{11}$$

$$\rho_a c_p \left(u_a \frac{\partial T_a}{\partial \xi} + \frac{v_a + \eta \tan \theta u_a}{\delta_a(x_1)} \frac{\partial T_a}{\partial \eta} \right)$$
$$= \frac{k_a}{\delta_a^2(x_1)} \left(\frac{\partial^2 T_a}{\partial \eta^2} \right) \tag{12}$$

$$u_a \frac{\partial W}{\partial \xi} + \frac{v_a + \eta \tan \theta u_a}{\delta_a(x_1)} \frac{\partial W}{\partial \eta} = \frac{D_a}{\delta_a^2(x_1)} \left(\frac{\partial^2 W}{\partial \eta^2} \right) \tag{13}$$

The general transformed mass, momentum, energy, and mass diffusion equations for air in the inclined counter flow channel can be written as

$$\left(\frac{\partial u_a}{\partial \xi} - \frac{\eta \tan \theta}{\delta_a(x_1)} \frac{\partial u_a}{\partial \eta} \right) + \frac{1}{\delta_a(x_1)} \frac{\partial v_a}{\partial \eta} = 0 \tag{14}$$

$$\rho_a \left(u_a \frac{\partial u_a}{\partial \xi} + \frac{v_a - \eta \tan \theta u_a}{\delta_a(x_1)} \frac{\partial u_a}{\partial \eta} \right)$$
$$= -\frac{\partial p}{\partial \xi} + \frac{\mu_a}{\delta_a^2(x_1)} \left(\frac{\partial^2 u_a}{\partial \eta^2} \right) \tag{15}$$

$$\rho_a \left(u_a \frac{\partial v_a}{\partial \xi} + \frac{v_a - \eta \tan \theta u_a}{\delta_a(x_1)} \frac{\partial v_a}{\partial \eta} \right)$$
$$= -\frac{\partial p}{\partial \eta} + \frac{\mu_a}{\delta_a^2(x_1)} \left(\frac{\partial^2 v_a}{\partial \eta^2} \right) \tag{16}$$

$$\rho_a c_p \left(u_a \frac{\partial T_a}{\partial \xi} + \frac{v_a - \eta \tan\theta u_a}{\delta_a(x_1)} \frac{\partial T_a}{\partial \eta} \right)$$
$$= \frac{k_a}{\delta_a^2(x_1)} \left(\frac{\partial^2 T_a}{\partial \eta^2} \right) \tag{17}$$

$$u_a \frac{\partial W}{\partial \xi} + \frac{v_a - \eta \tan\theta u_a}{\delta_a(x_1)} \frac{\partial W}{\partial \eta} = \frac{D_a}{\delta_a^2(x_1)} \left(\frac{\partial^2 W}{\partial \eta^2} \right) \tag{18}$$

The mass, momentum, energy, and mass diffusions equations for the desiccant film are given by

$$\frac{\partial u_d}{\partial x_2} = 0 \tag{19}$$

$$\rho_d g + \mu_d \left(\frac{\partial^2 u_d}{\partial y_2^2} \right) = 0 \tag{20}$$

$$\rho_d c_{pd} u_d \frac{\partial T_d}{\partial x_2} = \frac{\partial}{\partial y_2} \left([(k_{\mathrm{eff}} + k_{\mathrm{dis}}) \frac{\partial T_d}{\partial y_2} \right) \tag{21}$$

$$u_d \frac{\partial C}{\partial x_2} = D_d \frac{\partial^2 C}{\partial y_2^2} \tag{22}$$

2.1. Low air Reynolds number for the inclined parallel flow

Since air Reynolds number will be small, the ξ—momentum equation for the air can be simplified as

$$0 = -\frac{\partial p}{\partial \xi} + \mu \frac{\mu_a}{\delta_a^2(x_1)} \left(\frac{\partial^2 u_a}{\partial \eta^2} \right) \tag{23}$$

The boundary and interfacial conditions become:

$$T_a(0, \eta) = T_{ai} \quad W(0, \eta) = W_i \tag{24}$$

$$T_d(0, y_2) = T_{di} \quad C(0, y_2) = C_i \tag{25}$$

$$\frac{\partial u_a}{\partial \eta} = 0, \quad \frac{\partial T_a}{\partial \eta} = 0, \quad \frac{\partial W}{\partial \eta} = 0$$

$$\text{at } \eta = 0 \text{ and } 0 \leqslant \xi \leqslant \frac{H}{\cos\theta} \tag{26}$$

$$u_a(\xi, 1) = u_{d\ \mathrm{int}} \cos\theta \quad T_a(\xi, 1) = T_d(x_2, \delta_d)$$

$$W(\xi, 1) = W_{\mathrm{int}} \tag{27}$$

where W_{int} is the interfacial humidity ratio and is given as [13]:

$$W_{\mathrm{int}} = 0.62185 \frac{p_z}{(p_t - p_z)} \tag{28}$$

where p_z is equal to [14]:

$$p_z = p_{ws} \left(1.0 - 0.828Z - 1.496Z^2 + Z \frac{(T_{\mathrm{int}} - 40)}{350} \right) \tag{29}$$

$$u_d(x_2, 0) = 0 \quad T_d(x_2, 0) = T_w \tag{30a}$$

$$\frac{\partial C}{\partial y_2} = 0 \quad \text{at } y_2 = 0 \text{ and } 0 \leqslant x_2 \leqslant \frac{H}{\cos\theta} \tag{30b}$$

Due to the negligible shear stress from the air side, the interfacial conditions can be reduced to the following form:

$$\frac{\partial u_d}{\partial y_2} = 0 \quad \text{at } y_2 = \delta_d \text{ and } 0 \leqslant x_2 \leqslant \frac{H}{\cos\theta} \tag{31}$$

The energy balance equation at the interface is

$$k_a \sin\theta \frac{\partial T_a}{\partial \xi} + k_a \left(\frac{\eta \sin\theta \tan\theta + \cos\theta}{\delta_a(x_1)} \right) \frac{\partial T_a}{\partial \eta}$$
$$+ \rho_a D_a h_{fg} \left(\sin\theta \frac{\partial W}{\partial \xi} + \left(\frac{\eta \sin\theta \tan\theta + \cos\theta}{\delta_a(x_1)} \right) \frac{\partial W}{\partial \eta} \right)$$
$$= -k_d \frac{\partial T_d}{\partial y_2} \quad \text{at } \eta = 1, \ y_2 = \delta_d \ \& \ 0 \leqslant x_2, \ \xi \leqslant \frac{H}{\cos\theta}$$
$$\tag{32}$$

The mass balance at the interface becomes:

$$\rho_a D_a \left(\sin\theta \frac{\partial W}{\partial \xi} + \left[\frac{\eta \sin\theta \tan\theta + \cos\theta}{\delta_a(x_1)} \right] \frac{\partial W}{\partial \eta} \right)$$
$$= -\rho_d D_d \frac{\partial C}{\partial y_2} \quad \text{at } \eta = 1, \ y_2 = \delta_d \ \& \ 0 \leqslant x_2, \xi \leqslant \frac{H}{\cos\theta}$$
$$\tag{33}$$

The axial velocity for the air (u_a) can be obtained analytically with the appropriate boundary conditions:

$$u_a(\xi, \eta) = u_{d\ \mathrm{int}} \cos\theta + \frac{\delta_a^2(x_1)}{2\mu_a} \frac{\partial p}{\partial \xi} (\eta^2 - 1) \tag{34}$$

Also, the transverse velocity (v_a) can be also obtained analytically by using the analytical solution for air velocity and continuity Eq. (1):

$$v_a(\xi, \eta) = \left(\frac{\delta_a^3(x_1)}{2\mu_a} \frac{\partial^2 p}{\partial \xi^2} \right) \left(\eta - \frac{\eta^3}{3} \right) - \left(\frac{\delta_a^2(x_1) \tan\theta}{\mu_a} \right) \frac{\partial p}{\partial \xi} \eta \tag{35}$$

where first and second order pressure drops are equal to

$$\frac{\partial p(\xi)}{\partial \xi} = \frac{3u_{d\ \mathrm{int}} \cos\theta \mu_a}{\delta_a^2(x_1)} - \frac{3\mu_a \dot{m}_a}{2\rho_a \delta_a^3(x_1) B} \tag{36}$$

$$\frac{\partial^2 p(\xi)}{\partial \xi^2} = \frac{6u_{d\ \mathrm{int}} \sin\theta \mu_a}{\delta_a^3(x_1)} - \frac{9\mu_a \dot{m}_a \tan\theta}{2\rho_a \delta_a^4(x_1) B} \tag{37}$$

The desiccant film velocity and thickness are

$$u_d(y_2) = \frac{\rho_d g}{\mu_d} y_2 \left[\delta_d - \frac{y_2}{2} \right] \tag{38}$$

$$\delta_{\mathrm{d}} = \left[\frac{3\dot{m}_{\mathrm{d}} v_{\mathrm{d}}}{\rho_{\mathrm{d}} g} \right]^{1/3} \tag{39}$$

where $\dot{m}_{\mathrm{a}}$ and $\dot{m}_{\mathrm{d}}$ are mass flow rates of air and desiccant film, respectively.

2.2. Low air Reynolds number for the inclined counter flow:

The reduced form of ξ—momentum Eq. (23) in the inclined parallel flow channel will also be valid for the inclined counter flow channel. Since the air will be flowing upward rather than downward, some boundary conditions should be modified as follows:

$$u_{\mathrm{a}}(\xi, 1) = -u_{\mathrm{d\ int}} \cos\theta \tag{40}$$

The energy balance equation at the interface is

$$
\begin{aligned}
&-k_{\mathrm{a}} \sin\theta \frac{\partial T_{\mathrm{a}}}{\partial \xi} + k_{\mathrm{a}} \left(\frac{\cos\theta + \eta \sin\theta \tan\theta}{\delta_{\mathrm{a}}(x_1)} \right) \frac{\partial T_{\mathrm{a}}}{\partial \eta} \\
&+ \rho_{\mathrm{a}} D_{\mathrm{a}} h_{\mathrm{fg}} \left(-\sin\theta \frac{\partial W}{\partial \xi} + \left(\frac{\cos\theta + \eta \sin\theta \tan\theta}{\delta_{\mathrm{a}}(x_1)} \right) \frac{\partial W}{\partial \eta} \right) \\
&= -k_{\mathrm{d}} \frac{\partial T_{\mathrm{d}}}{\partial y_2} \quad \text{at } \eta = 1,\ y_2 = \delta_{\mathrm{d}}\ \&\ 0 \leqslant x_2\ \&\ \xi \leqslant \frac{H}{\cos\theta}
\end{aligned}
\tag{41}
$$

The mass balance at the interface becomes:

$$
\begin{aligned}
&\rho_{\mathrm{a}} D_{\mathrm{a}} \left(-\sin\theta \frac{\partial W}{\partial \xi} + \left(\frac{\cos\theta + \eta \sin\theta \tan\theta}{\delta_{\mathrm{a}}(x_1)} \right) \frac{\partial W}{\partial \eta} \right) \\
&= -\rho_{\mathrm{d}} D_{\mathrm{d}} \frac{\partial C}{\partial y_2} \quad \text{at } \eta = 1,\ y_2 = \delta_{\mathrm{d}}\ \&\ 0 \leqslant x_2\ \&\ \xi \leqslant \frac{H}{\cos\theta}
\end{aligned}
\tag{42}
$$

The axial and transverse velocities can be obtained analytically for the inclined counter flow channels:

$$u_{\mathrm{a}}(\xi, \eta) = -u_{\mathrm{d\ int}} \cos\theta + \frac{\delta_{\mathrm{a}}^2(x_1)}{2\mu_{\mathrm{a}}} \frac{\partial p}{\partial \xi}(\eta^2 - 1) \tag{43}$$

$$v_{\mathrm{a}}(\xi, \eta) = \left(\frac{\delta_{\mathrm{a}}^3(x_1)}{2\mu_{\mathrm{a}}} \frac{\partial^2 p}{\partial \xi^2} \right) \left(\frac{\eta^3}{3} - \eta \right) - \left(\frac{\delta_{\mathrm{a}}^2(x_1) \tan\theta}{\mu_{\mathrm{a}}} \right) \frac{\partial p}{\partial \xi} \eta \tag{44}$$

$$\frac{\partial p(\xi)}{\partial \xi} = -\frac{3\mu_{\mathrm{a}} \dot{m}_{\mathrm{a}}}{2\rho_{\mathrm{a}} \delta_{\mathrm{a}}^3(x_1) B} - \frac{3u_{\mathrm{d\ int}} \cos\theta \mu_{\mathrm{a}}}{\delta_{\mathrm{a}}^2(x_1)} \tag{45}$$

$$\frac{\partial^2 p(\xi)}{\partial \xi} = \frac{6 u_{\mathrm{d\ int}} \sin\theta \mu_{\mathrm{a}}}{\delta_{\mathrm{a}}^3(x_1)} + \frac{9\mu_{\mathrm{a}} \dot{m}_{\mathrm{a}} \tan\theta}{2\rho_{\mathrm{a}} \delta_{\mathrm{a}}^4(x_1) B} \tag{46}$$

2.3. High air Reynolds number for the inclined parallel flow

The vorticity equation and stream function are introduced to solve for high air Reynolds number cate-

gory. These equations in the transformed domain are given by

$$u_{\mathrm{a}} \frac{\partial \Omega}{\partial \xi} + \frac{v_{\mathrm{a}} + \eta \tan\theta u_{\mathrm{a}}}{\delta_{\mathrm{a}}(x_1)} \frac{\partial \Omega}{\partial \eta} = \frac{v_{\mathrm{a}}}{\delta_{\mathrm{a}}^2(x_1)} \left(\frac{\partial^2 \Omega}{\partial \eta^2} \right) \tag{47}$$

$$\frac{1}{\delta_{\mathrm{a}}^2(x_1)} \frac{\partial^2 \psi}{\partial \eta^2} = -\Omega \tag{48}$$

Both components of velocities can be solved from the vorticity and stream functions by the following equations:

$$\Omega = -\frac{1}{\delta_{\mathrm{a}}(x_1)} \frac{\partial u_{\mathrm{a}}}{\partial \eta} \tag{49}$$

$$u_{\mathrm{a}} = \frac{1}{\delta_{\mathrm{a}}(x_1)} \frac{\partial \psi}{\partial \eta} \tag{50a}$$

$$v_{\mathrm{a}} = -\left(\frac{\partial \psi}{\partial \xi} + \frac{\eta \tan\theta}{\delta_{\mathrm{a}}(x_1)} \frac{\partial \psi}{\partial \eta} \right) \tag{50b}$$

The following boundary conditions are imposed:

$$\Omega(0, \eta) = 0 \tag{51a}$$

$$\Omega(\xi, 0) = 0 \quad \psi(\xi, 0) = 0 \tag{51b}$$

$$\Omega(\xi, 1) = -\frac{1}{\delta_{\mathrm{a}}(x_1)} \frac{\partial u_{\mathrm{a}}}{\partial \eta} \Big|_{\eta=1} \quad \psi(\xi, 1) = \frac{Q_{\mathrm{a}}}{2} \tag{51c}$$

where Q_{a} is volume flow rate of the air.

The energy and mass diffusion equations remain the same as for the parallel flow low Reynolds number flow case.

2.4. High air Reynolds number for the inclined counter flow

The vorticity equation will be slightly different than the inclined parallel flow because of the change in the definition of the air thickness (Eqs. (7) and (8)) and it can be cast as

$$u_{\mathrm{a}} \frac{\partial \Omega}{\partial \xi} + \frac{v_{\mathrm{a}} - \eta \tan\theta u_{\mathrm{a}}}{\delta_{\mathrm{a}}(x_1)} \frac{\partial \Omega}{\partial \eta} = \frac{v_{\mathrm{a}}}{\delta_{\mathrm{a}}^2(x_1)} \left(\frac{\partial^2 \Omega}{\partial \eta^2} \right) \tag{52}$$

The definition of velocity in the transverse direction is slightly changed to

$$v_{\mathrm{a}} = -\left(\frac{\partial \psi}{\partial \xi} - \frac{\eta \tan\theta}{\delta_{\mathrm{a}}(x_1)} \frac{\partial \psi}{\partial \eta} \right) \tag{53}$$

The boundary conditions for the vorticity and stream functions will remain the same as for the parallel flow high air Reynolds number case.

2.5. Analysis of ultrafine particles in the desiccant film

The conventional approach and modified conventional approach are used by Xuan and Roetzel [12] to

estimate the thermal conductivity of the solid–liquid mixture. Both approaches are utilized in this study. The $(\rho C_p)_{eff}$ of the nanofluids can be computed as

$$(\rho c_p)_{eff} = (1 - \phi)(\rho c_p)_f + \phi(\rho c_p)_s \tag{54}$$

where ϕ is the partial volume fraction and defined as [15]:

$$\phi = \frac{V_s}{V_f + V_s} = N \frac{\pi}{6} d_s^3 \tag{55}$$

Brinkman [16] extended Einstein's equation for effective fluid viscosity as

$$\mu_{eff} = \mu_f \frac{1}{(1 - \phi)^{2.5}} \tag{56}$$

A relationship was developed by Hamilton and Crosser [17] to calculate the thermal conductivity of solid–liquid mixture which is valid for thermal conductivity ratio larger than 100:

$$\frac{k_{eff}}{k_f} = \frac{k_s + (n-1)k_f - (n-1)\phi(k_f - k_s)}{k_s + (n-1)k_f + \phi(k_f - k_s)} \tag{57}$$

where k_{eff} in the above equation is considered for conventional single-phase fluid (conventional approach) and n is an empirical factor and defined as

$$n = 3/\psi \tag{58}$$

where Ψ is the sphericity.

Xuan and Roetzel [12] suggested that dispersed thermal conductivity of the nanofluids (modified conventional approach) may be obtained using the dispersed thermal conductivity for a porous medium [18,19]:

$$k_{dis} = \lambda(\rho c_p)_{eff} u_d \tag{59}$$

where a new constant, λ, is introduced, called coefficient of thermal dispersion coefficent, and defined as

$$\lambda = C d_p R \phi \tag{60}$$

where C is a constant, d_p the diameter of the particles, and R is radius of the tube.

The properties of air are obtained from ASHRAE handbook of fundamentals [13]. Calcium chloride solution is used as desiccant film and its properties are taken from calcium chloride properties handbook [20] and the properties of Cu-ultrafine particles are obtained from Eastman et al. [21].

It should be noted that ultrafine particles (nanometer) in fluids are a new technology under development. There are still no substantial experimental work or established theory to estimate the thermal conductivity of ultrafine particles in fluids. Xuan and Li [15] used the Hamilton and Crosser model to estimate the thermal conductivity of ultrafine particles in fluids and a good

agreement was achieved with the experimental data at $\psi = 0.7$ where ψ is the sphericity. In another study, Lee et al. [11] found that the predicted thermal conductivity of Al_2O_3 ultrafine particles in fluid was in a good agreement with the experimental results at $\psi = 1.0$. Therefore, the Hamilton and Crosser model can be extended to predict the thermal conductivity of ultrafine particles in fluids. In the literature, there is no definitive work in the thermal dispersion of ultrafine particles in fluids. Xuan and Roetzel [12] assumed that dispersed thermal conductivity of ultrafine particles in fluids might be approximated as thermal dispersion in porous media.

2.6. Calculated parameters

The air and desiccant film Reynolds numbers are defined as

$$Re_a = \frac{4\rho_a u_{am}(x_1)\delta_a(x_1)}{\mu_a} \tag{61}$$

$$Re_d = \frac{4\rho_d u_{dm}\delta_d}{\mu_d} \tag{62}$$

The exit air and desiccant conditions are calculated based on the mean bulk values Γ_{ao}, Γ_{do} and can be written as

$$\Gamma_{ao} = \frac{\int_0^1 u_a \Gamma \, d\eta}{\int_0^1 u_a \, d\eta} \tag{63}$$

$$\Gamma_{do} = \frac{\int_0^{\delta_d} u_d \Gamma \, dy_2}{\int_0^{\delta_d} u_d \, dy_2} \tag{64}$$

where Γ_a can be temperature or humidity ratio for the air and Γ_d can be either temperature or concentration of desiccant film.

3. Numerical analysis

The velocity profiles for parallel and counter flow for low air Reynolds numbers are solved analytically while the energy and mass diffusion equations are solved numerically. The axial convection terms are approximated by first order upwind differencing while transverse convection and diffusion terms are approximated by first and second order central differencing, respectively. An iterative method is employed to satisfy the interfacial conditions between air and the desiccant film. A transient approach is utilized for the vorticity equation for high Reynolds number cases. Alternating direction implicit method is used for the vorticity equation and the stream function is solved by successive over-relaxation method. Fig. 2(a) shows a good agreement between centerline velocities for inclined parallel flow channel for low (analytical) and high Reynolds number cases for different inclination angles. As illustrated in Fig. 2(b), a
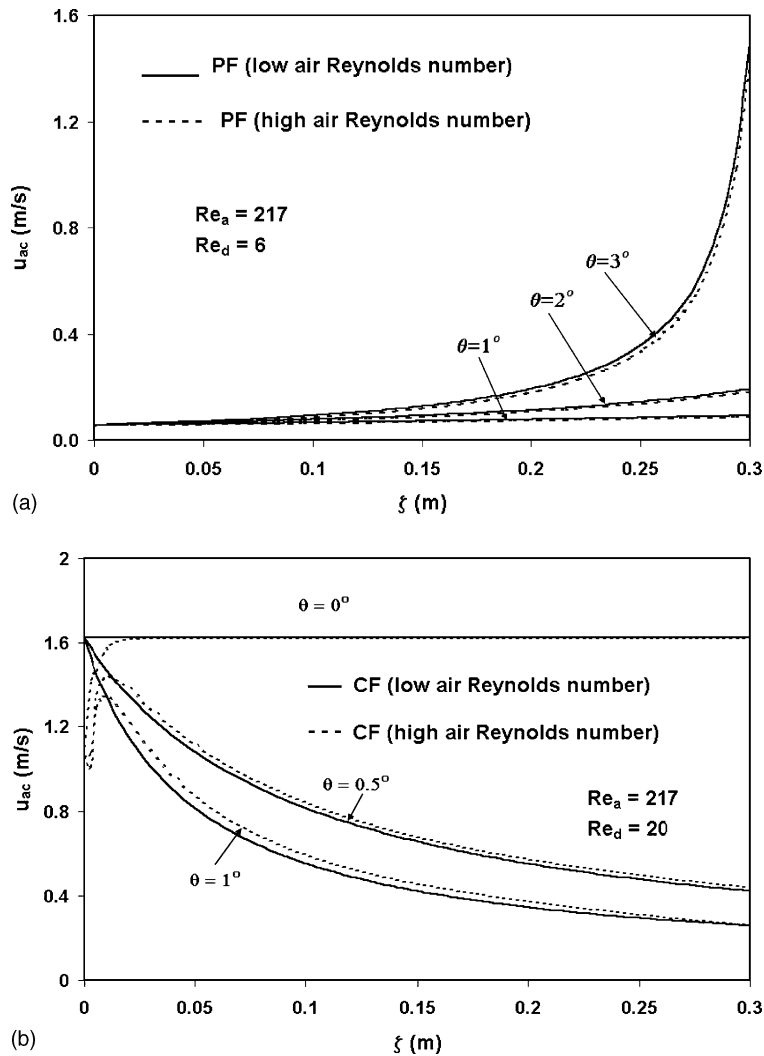
Fig. 2. Comparison between for the centerline velocities for low and high air Reynolds number categories (a) inclined parallel flow channel and (b) inclined counter flow configuration.

good agreement is also achieved for the centerline velocity for the low and high Reynolds number cases for the inclined counter flow configurations. It should be noted that the discrepancy in the results for small values of ξ is due to the neglect of the convective terms in obtaining the analytical solution for low Reynolds number case.

4. Results and discussion

A parametric study is employed to investigate the dehumidification and cooling processes for the air and the regeneration process for the desiccant film. Three different categories are parametrically investigated in this study: low air Reynolds number for the inclined parallel flow and counter flow channels and high air

Reynolds number for the inclined parallel flow configuration. This study is mainly focused on the effect of inclination angle on heat and mass transfer between air and desiccant film.

4.1. Low air Reynolds number flow

Dehumidification and cooling processes for inclined parallel and counter flow channels at different air and desiccant Reynolds numbers for different inclination angles are investigated.

4.1.1. Effect of the air Reynolds number
In the inclined parallel flow channel, the exit air temperature and humidity ratio increases with an increase in the air Reynolds number for different inclination

angles, as shown in Fig. 3(a) and (b). The humid air would have less time to be in contact with desiccant film at high air Reynolds number. However, the increase in the inclination angle causes a large boost in the air velocity especially down the channel, which results in higher convection rates for both the energy and mass diffusion equations for the air and consequently an increase in the heat and mass transfer between the air and the desiccant film. This yields an overall reduction in the exit air temperature and humidity ratio. For the inclined counter flow configuration, the inlet effect of the desiccant film has a dominant effect in increasing the overall exit air temperature. However, the exit air temperature and humidity ratio decreases with an increase in the air Reynolds number due to the fact that effects of inlet desiccant conditions are reduced at higher air Reynolds

numbers. The overall exit air temperature and humidity ratio decreases at higher inclination angle due to an increase in the channel width at higher inclination angle further reducing inlet desiccant effects. The inclination angle plays a significant role in enhancing the dehumidification and cooling processes for air for both flow regimes.

4.1.2. Effect of the desiccant Reynolds number

The desiccant Reynolds number with inclination has a noticeable effect on the dehumidification and cooling processes of the air. For the inclined parallel flow regime, heat and mass transfer coefficients increase with an increase in the desiccant Reynolds number, this in turn results in an increase in the heat and mass transfer between the air and the desiccant film and a decrease in
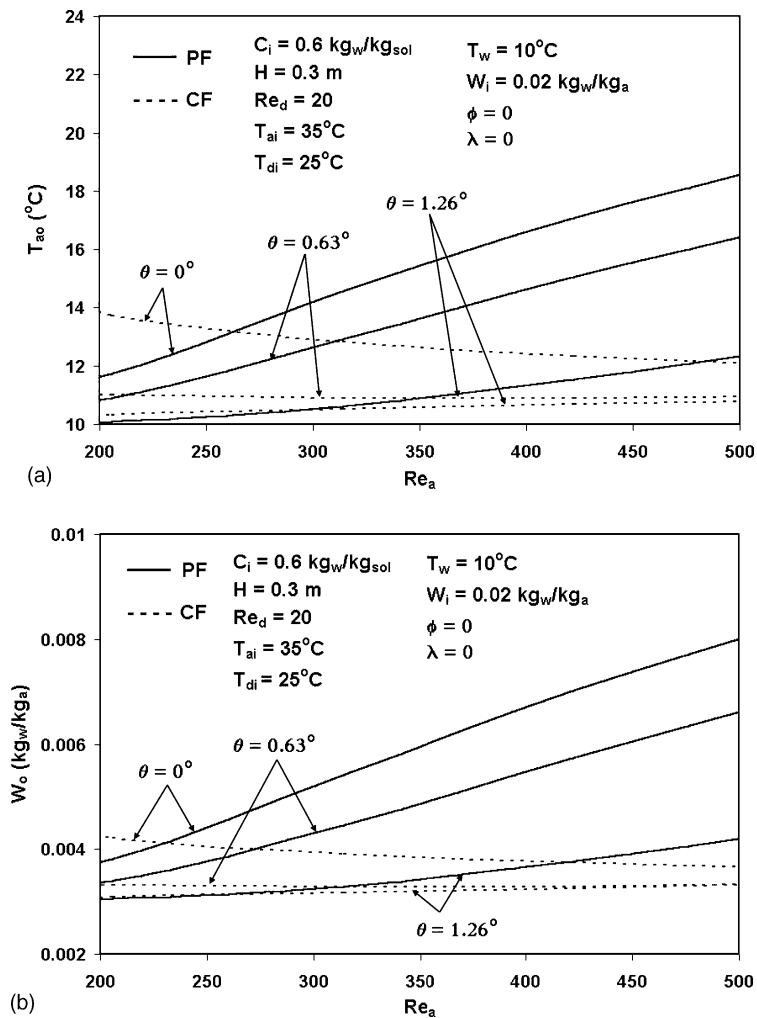

Fig. 3. Effect of air Reynolds number (Low flow category) for the inclined parallel and counter flow configurations on (a) exit air temperature and (b) exit humidity ratio.

exit air conditions, as shown in Fig. 4(a). However, these enhancements are modest due to the small thickness of the film. In the inclined counter flow channel, Fig. 4(b) once again shows that the inlet desiccant conditions play a significant role in increasing the exit air conditions. It is important to note that the inclination angle plays a vital role in reducing the overall exit temperature and humidity ratio for both flow arrangements.

4.2. High air Reynolds number flow

In what follows the effect of inclination angle on heat and mass transfer between air and desiccant film for the dehumidification and cooling processes for the air and regeneration process of liquid desiccant in terms of pertinent parameters is investigated.

4.2.1. Effect of the air inlet conditions

An increase in the inlet air temperature with the inclination angle has a significant effect on heat and mass transfer between air and desiccant film. Fig. 5 shows that an increase in the inclination angle up to 2° results a reduction up to 25% in the exit air temperature and 34% in the exit humidity ratio, respectively. The increase in the inclination angle causes an increase in the surface contact area between air and desiccant film which allows more heat and mass transfer between them. Also, it results in an increase in the velocity profile of the air down the channel which results in an increase in convection rates in the energy and mass diffusion equations of the air and therefore an overall reduction in exit air conditions. In addition, an increase in the inlet air temperature causes an increase the saturated pressure
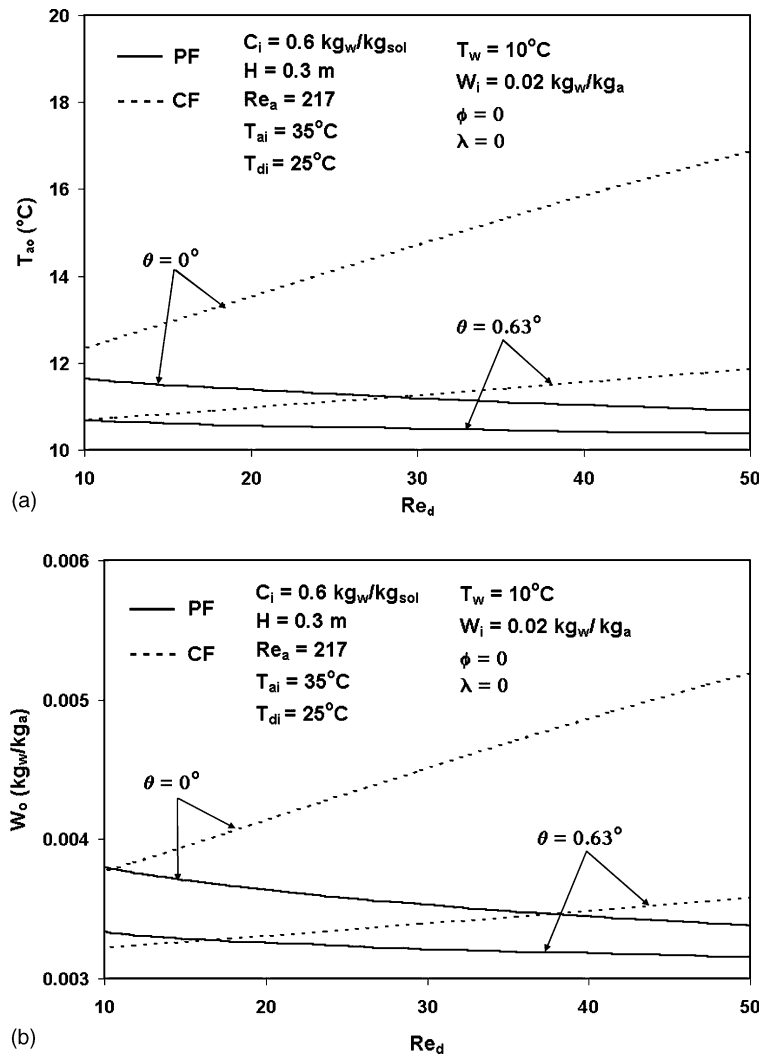

Fig. 4. Effect of desiccant Reynolds number (low flow category) for the inclined parallel and counter flow configurations on (a) exit air temperature and (b) exit humidity ratio.
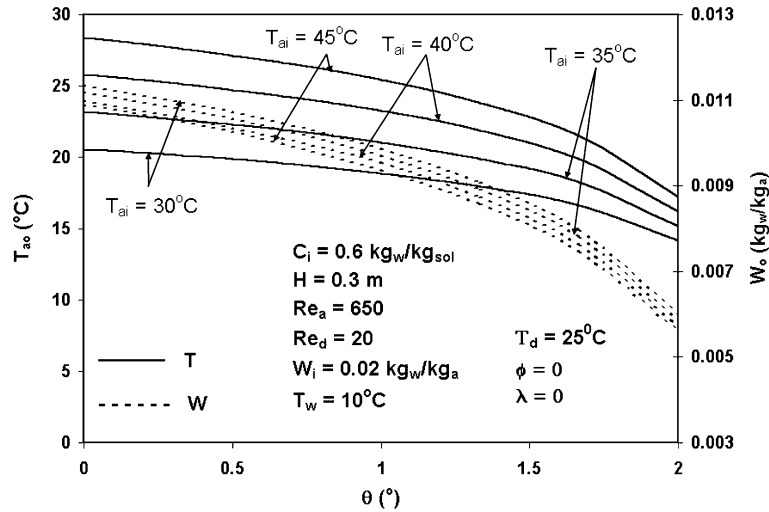
Fig. 5. Effect of inlet air temperature for the inclined parallel flow channel on exit air conditions.

difference between moist air and desiccant film, which in turn causes an increase in the mass transfer rate from the air to the desiccant film and a further decrease in the exit humidity ratio.

4.2.2. Effect of the film inlet conditions

The variation in inlet desiccant temperature with inclination has some significance on the dehumidification and cooling processes. Fig. 6 shows that the change in inlet desiccant temperature does not have an impact on exit air conditions. However, the inclination angle plays a significant role in reducing the exit air conditions which results in better dehumidification and cooling processes.

The variation in the inlet concentration of liquid solution does not change the exit air temperature, as illustrated in Fig. 7, but it reduces the exit humidity ratio. A decrease in the inlet concentration of desiccant film causes an increase in the salt solution of the desiccant, which in turn increases the saturated pressure difference between the air and the film and allows more mass transferred from the air to the film. The inclination angle reduces the exit air temperature because of the increase in the contact surface area and convection rates. Dehumidification process is enhanced at low concentration of desiccant film; however cooling process is not affected by altering film concentration.
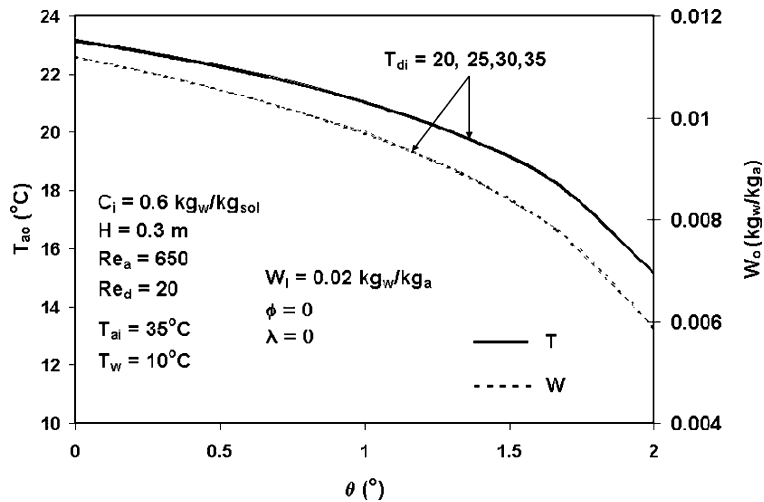

Fig. 6. Effect of inlet desiccant temperature for the inclined parallel flow channel on exit air conditions.
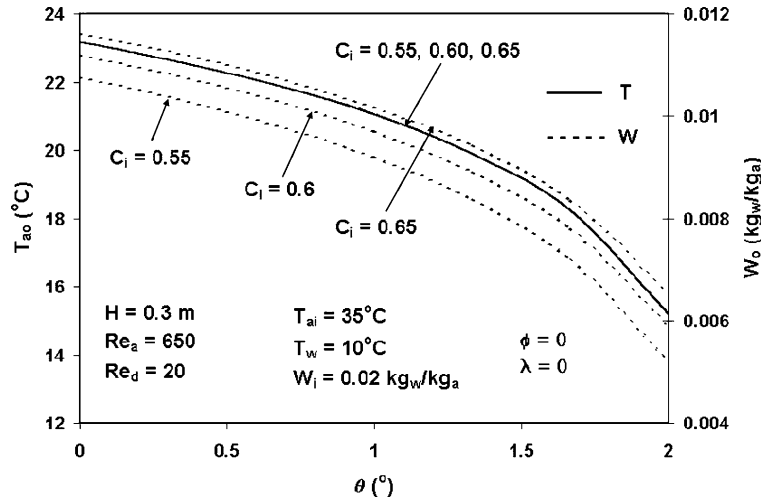
Fig. 7. Effect of inlet desiccant concentration for the inclined parallel flow channel on exit air conditions.

4.2.3. Effect of the air Reynolds number

The exit concentration of liquid desiccant decreases at high Reynolds number is illustrated in Fig. 8. It can be seen that an increase in the inclination angle enhances the regeneration process by lowering the overall exit concentration of the desiccant film. This is mainly due to an increase in the contact surface area, which in turn allows more mass transfer from liquid desiccant to the hot air and an increase in the air velocity resulting in a boost in convection.

4.2.4. Effect of the desiccant Reynolds number

The desiccant film would have less time to be in contact with the air at high desiccant Reynolds numbers resulting in less mass transfer from the desiccant film to

the air and higher exit concentration for the liquid desiccant, as shown in Fig. 9. In addition, the inclination angle plays a role in reducing the exit concentration of the desiccant film which enhances the liquid desiccant regeneration process due to an increase in the contact surface area and higher convection rates. Therefore, low desiccant Reynolds number with higher inclination angle provides better regeneration process for the desiccant film.

4.2.5. Effect of variation in the Cu-ultrafine particles volume fraction

The addition of Cu-ultrafine particles increases the thermal conductivity of the desiccant film, as shown in Fig. 10. Fig. 10 also shows that the film thickness
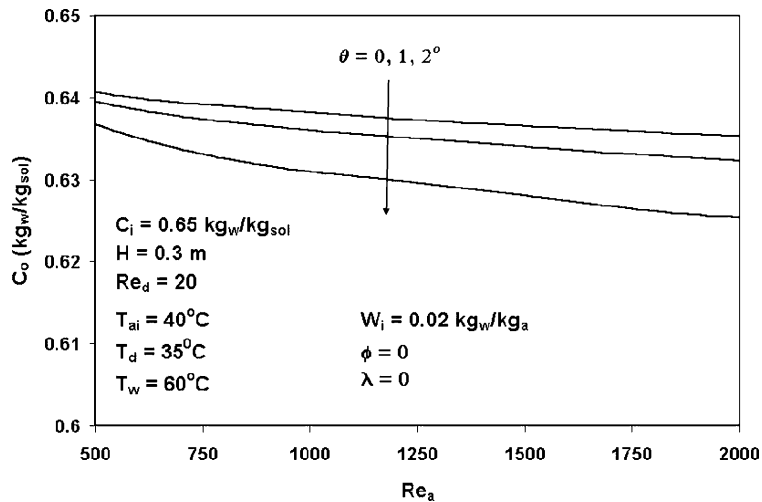

Fig. 8. Effect of air Reynolds number for regeneration process of liquid desiccant for the inclined parallel flow channel on exit concentration of desiccant film.
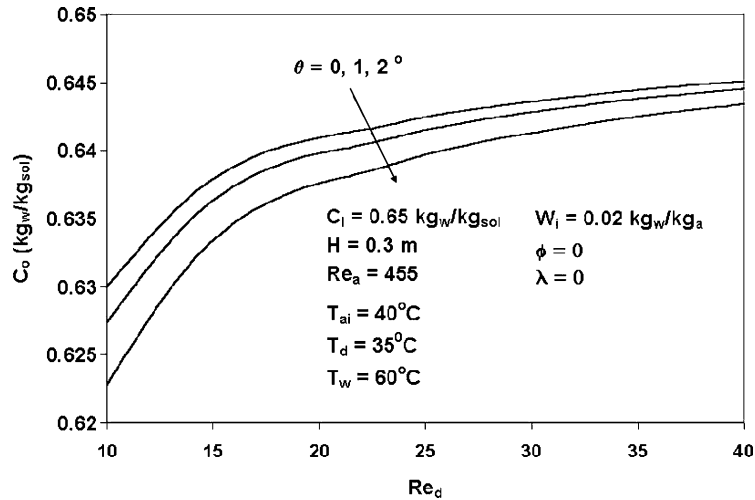
Fig. 9. Effect of desiccant Reynolds number for regeneration process of liquid desiccant for the inclined parallel flow channel on exit concentration of desiccant film.
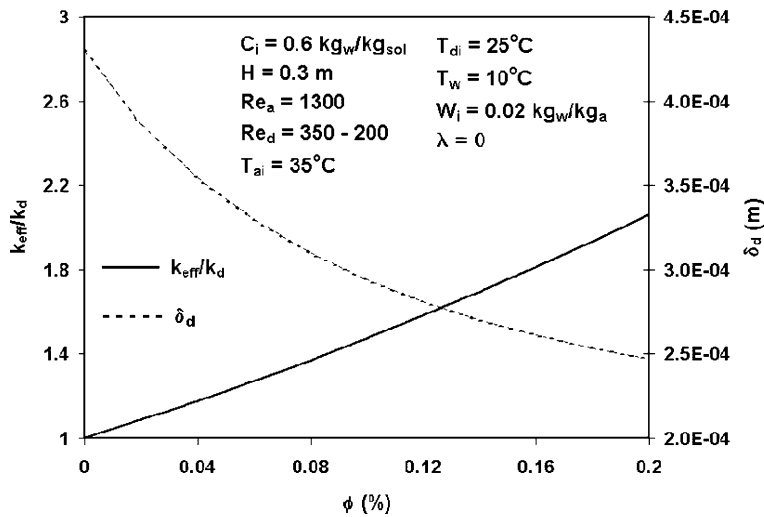
Fig. 10. Effect of Cu-ultrafine particles volume fraction in liquid desiccant on ratio of effective thermal conductivity to thermal conductivity of liquid desiccant and film thickness.

decreases with an increase in the volume fraction due to an increase in the effective density of the liquid solution. As expected, an increase in the volume fraction results in an increase in the heat transfer between air and desiccant film which results in lower exit air temperature, but no significant reduction is noticed in the exit humidity ratio, as seen in Fig. 11. It is also important to note that the reduction in the exit air temperature is modest ($\cong 5\%$) due to the small thickness of the desiccant film. The inclination angle once again plays a significant role in reducing both exit air temperature and the humidity ratio. Therefore, both dehumidification and cooling processes are improved by an increase in the inclination

angle, but only cooling process of air has a noticeable enhancement by addition of the Cu-ultrafine particles volume fraction.

The exit concentration of the desiccant film almost stays constant with an increase in the volume fraction of Cu-ultrafine particles, as seen in Fig. 12. However, the inclination angle reduces the overall exit concentration of the desiccant film.

4.2.6. Effect of thermal dispersion

An increase in the thermal dispersion reduces the exit air temperature, as shown in Fig. 13. However, these reductions are very small due to the small thickness of
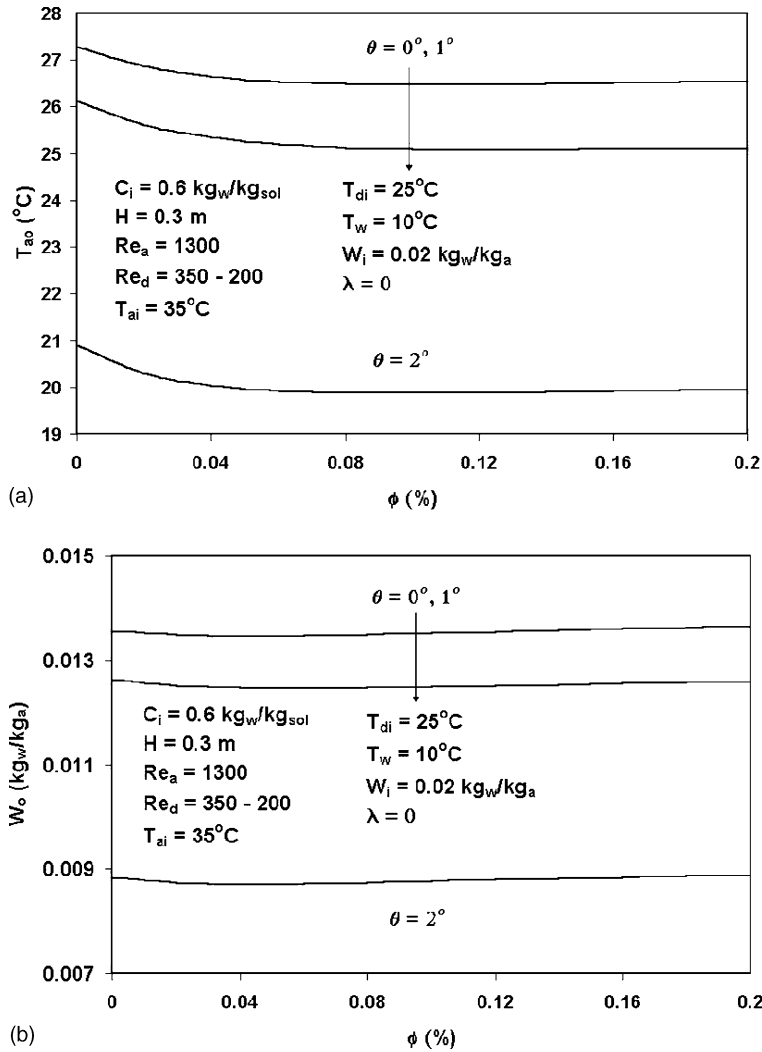
Fig. 11. Effect of Cu-ultrafine volume fraction in liquid desiccant in dehumidification and cooling processes of air on (a) exit air temperature and (b) exit humidity ratio.

the desiccant film compared with the thickness of the moist air. As expected, the inclination angle substantially reduces the exit air conditions. Therefore, the dehumidification and cooling processes are enhanced by the presence of the thermal dispersion of Cu-ultrafine particles in the desiccant film.

There is no noticed change in the exit concentration of liquid desiccant due to its small thickness, as seen in Fig. 14. Therefore, the regeneration process of liquid desiccant is not affected by the thermal dispersion effects, but enhanced by increasing the inclination angle. It should be noted that the addition of Cu-ultrafine particles boosts the effective thermal conductivity of solid–liquid mixture as shown in Fig. 10. However, the enhancements in the dehumidification, cooling, and regeneration processes are very minimal due the small thickness of the film compared to the thickness of the air as seen in Figs. 11–14.

5. Conclusions

Heat and mass transfer between the air and desiccant film for an inclined parallel and counter flow channels is investigated. Effect of the inclination angle is examined to study enhancement in dehumidification and cooling processes of air and regeneration of liquid desiccant in terms of pertinent parameters. The main conclusions of this investigation are
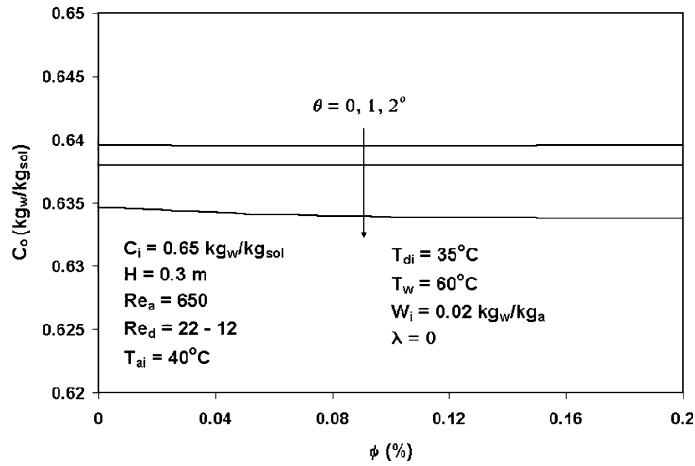
Fig. 12. Effect of Cu-ultrafine volume fraction on the liquid desiccant in regeneration process on exit concentration of desiccant film.
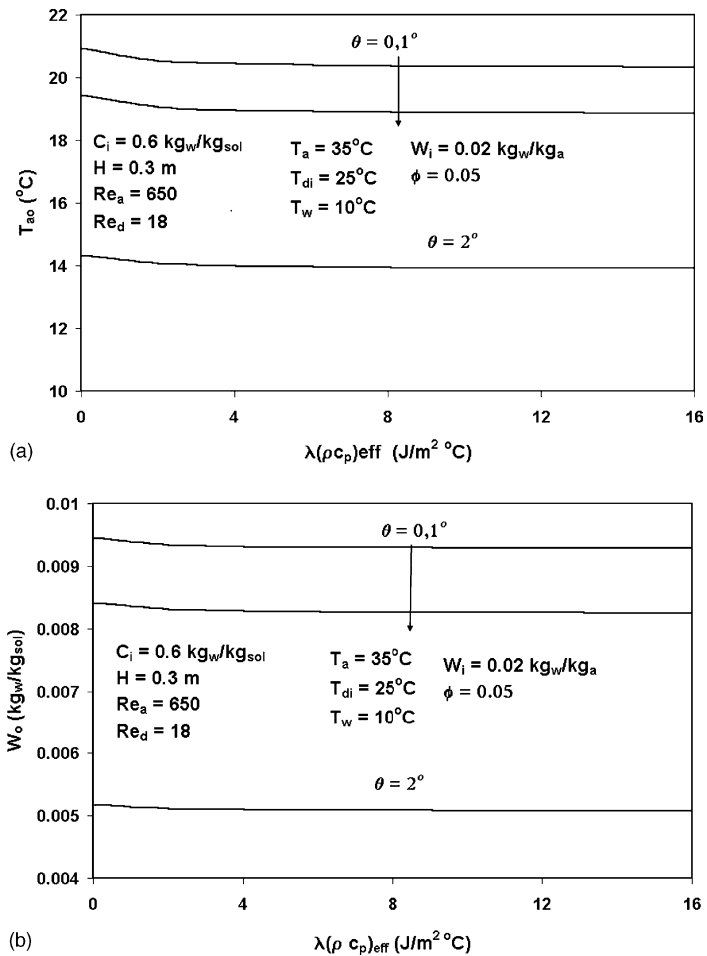
Fig. 13. Effect of thermal dispersion of Cu-ultrafine particles in liquid desiccant on dehumidification and cooling processes of air in terms of (a) exit air temperature and (b) exit humidity ratio.
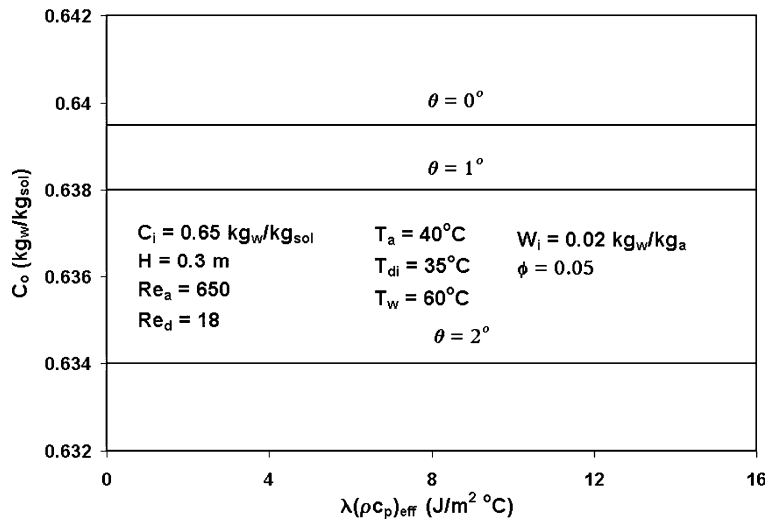
Fig. 14. Effect of thermal dispersion of Cu-ultrafine particles on the exit concentration of desiccant film.

1. Inclination angle plays a significant role in improving dehumidification and cooling processes of the air and regeneration process of liquid desiccant for both inclined parallel and counter flow channels.
2. Dehumidification and cooling processes are enhanced at low air Reynolds numbers while the liquid desiccant regeneration process is enhanced at high air Reynolds number.
3. Low desiccant flow enhances the regeneration process and high desiccant flow augments the dehumidification and cooling processes in an inclined parallel flow channel.
4. High inlet air temperature and low desiccant inlet concentration produce better dehumidification process.
5. An increase in the volume fraction and thermal dispersion increases the effective thermal conductivity of liquid desiccant, however, enhancements in dehumidification, cooling, regeneration processes are minimal due to the small thickness of desiccant film.

References

[1] J.R. Howel, J.L. Peterson, Preliminary performance evaluation of a hybrid vapor compression/liquid desiccant air conditioning system, ASME, Anaheim, Ca, 1986, Paper 86-WA/Sol. 9.

[2] J.W. Studak, J.L. Perterson, A preliminary evaluation of alternative liquid desiccants for a hybrid desiccant air conditioner, in: Proceedings of the Fifth Annual Symposium on Improving Building Energy Efficiency in Hot and Humid Climates, Houston, TX, vol. 13–14, 1988, pp. 155–159.

[3] F. Sick, T.K. Bushulte, S.A. Klein, P. Northey, J.A. Duffie, Analysis of the seasonal performance of hybrid desiccant cooling systems, Solar Energy 40 (3) (1988) 211–217.

[4] G.O. Lof, House heating and cooling with solar energy, in: Solar Energy Research, University of Wisconsin, Madison, USA, 1955.

[5] A. Chraibi, A. Jaffrin, S. Makhlouf, N. Bentounes, Dehumidifying Greenhouse air by direct cross-current contact with an organic desiccant liquid, J. Phys. 5 (7) (1995) 1055–1074.

[6] A.A. Al-Farayedhi, P. Gandhidasan, M.A. Al-Mutairi, Evaluation of heat and mass transfer coefficient in a gauze-type structured packing air dehumidifier operating with liquid desiccant, Int. J. Refrig. 25 (3) (2002) 330–339.

[7] A. Ali, K. Vafai, A.-R.A. Khaled, Comparative study between parallel and counter flow configurations between air and falling film desiccant with the presence of nanoparticles suspensions, Int. J. Energy Res. 27 (8) (2003) 725–745.

[8] A. Ali, K. Vafai, A.-R.A. Khaled, Analysis of heat and mass transfer between air and falling film in a cross flow configuration, Int. J. Heat Mass Transfer 47 (2004) 743–755.

[9] J.A. Eastman, S.U. Choi, W. Yu, L.J. Thompson, Anomalously increased effective thermal conductivities of ethylene glycol-based nanofluids containing copper nanoparticles, Appl. Phys. Lett. 78 (6) (2001) 718–720.

[10] S. Choi, Enhancing thermal conductivity of fluids with nanoparticles, ASME FED 231 (1995) 100–103.

[11] S. Lee, U.S. Choi, S. Li, J.A. Eastman, Measuring thermal conductivity of fluids containing oxide nanoparticles, J. Heat Transfer 121 (2) (1999) 280–289.

[12] Y. Xuan, W. Roetzel, Conceptions for heat transfer correlation of nanofluids, Int. J. Heat Mass Transfer 43 (19) (2000) 3701–3707.

[13] ASHRAE Handbook of Fundamentals, SI ed., American Society of Heating, Refrigeration, and Air-Conditioning, 1989.

[14] A. Rahmah, Heat and mass transfer between air and a falling film of desiccant solution in a fin-tube arrangement. M.S. Thesis, Kuwait University, Kuwait, 1997.

[15] Y. Xuan, Q. Li, Heat transfer enhancement of nanofluids, Int. J. Heat Fluid Flow 21 (1) (2000) 58–64.

[16] H.C. Brinkman, Viscosity of concentrated suspensions and solutions, J. Chem. Phys. 20 (1952) 571–581.

[17] R.L. Hamilton, O.K. Crosser, Thermal conductivity of heterogeneous two-component system, IEC Fund. 1 (1962) 182–191.

[18] M.L. Hunt, C.L. Tien, Effect of thermal dispersion on forced convection in fibrous media, Int. J. Heat Mass Transfer 31 (2) (1988) 301–309.

[19] A. Amiri, K. Vafai, Analysis of dispersion effects and non-thermal equilibrium non-Darcian variable porosity incompressible flow through porous medium, Int. J. Heat Mass Transfer 37 (6) (1994) 939–954.

[20] Dow Chemical Company, Calcium Chloride Properties and Forms Handbook, Dow Chemical Company, Midland, Michigan, 1983.

[21] J.A. Eastman, U.S. Choi, S. Li, L.J. Thompson, in: S. Komarnenl, J.C. Parker, H.C. Wollenberger (Eds.), Nanocrystalline and Nanocomposite Materials II, vol. 457, Materials Research Society, Pittsburgh, PA, 1997, pp. 3–11.